



Synthesis and characterization of biphenyl-based azo liquid crystals and its optical properties: effect of lateral and tail group

Akshay Thakor, Durgesh J. Dwivedi, Vipul Desai, Upendra H. Jadeja, Vinay S. Sharma & R. B. Patel

To cite this article: Akshay Thakor, Durgesh J. Dwivedi, Vipul Desai, Upendra H. Jadeja, Vinay S. Sharma & R. B. Patel (2021): Synthesis and characterization of biphenyl-based azo liquid crystals and its optical properties: effect of lateral and tail group, Molecular Crystals and Liquid Crystals, DOI: [10.1080/15421406.2021.1933685](https://doi.org/10.1080/15421406.2021.1933685)

To link to this article: <https://doi.org/10.1080/15421406.2021.1933685>



Published online: 26 Jun 2021.



Submit your article to this journal [↗](#)



Article views: 14



View related articles [↗](#)



View Crossmark data [↗](#)



Synthesis and characterization of biphenyl-based azo liquid crystals and its optical properties: effect of lateral and tail group

Akshay Thakor^a, Durgesh J. Dwivedi^a, Vipul Desai^a, Upendra H. Jadeja^b,
Vinay S. Sharma^c, and R. B. Patel^a

^aDepartment of Chemistry, K.K. Shah Jarodwala Maninagar Science College, Gujarat University, Ahmedabad, Gujarat, India; ^bDepartment of Chemistry, President Science College, Gujarat University, Ahmedabad, Gujarat, India; ^cDepartment of Chemistry, Faculty of Basic and Applied Science, Madhav University, Sirohi, Rajasthan, India

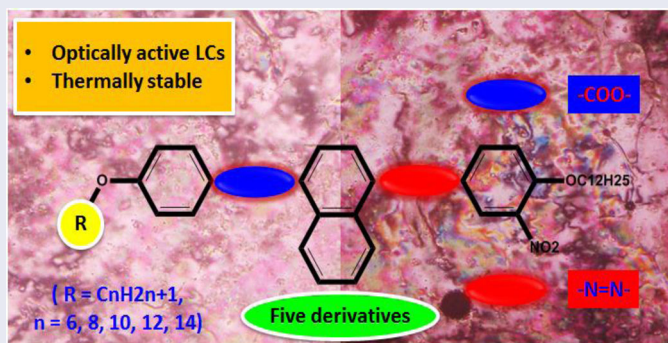
ABSTRACT

An azo ester-based biphenyl substituted rod-shaped azo-based material has been synthesized and well-characterized and further studied their mesogenic, optical, and thermal properties. All the synthesized derivatives displayed enantiotropical nematic and SmC phases with good temperature range of mesophase which is further influence by the variation of alkyl chain. The present synthesized derivatives having left terminally substituted phenyl ring by -OR inbuilt with ester azo group and right terminally dodecyloxy tail (-OC₁₂H₂₅) at the right terminal end. The mesomorphism is measured by using POM, DSC, and high-temperature XRD technique, and the photophysical behavior was measured by UV-Vis spectroscopy.

KEYWORDS

Azo; liquid crystal; nematic; smectic C; thermotropic

GRAPHICAL ABSTRACT



1. Introduction

A unique physical state of matter termed as liquid crystal (LC) or mesomorphic or mesogenic state [1] which is neither fully solid crystalline nor fully isotropic liquid is useful in the manufacture of electronic display devices, light-emitting materials, and

CONTACT Akshay Thakor ✉ akkythakor2901@gmail.com 📧 Department of Chemistry, K.K. Shah Jarodwala Maninagar Science College, Gujarat University, Ahmedabad-380009, Gujarat, India.

© 2021 Taylor & Francis Group, LLC

other electronic applications. Azo dyes are equally useful as normal dyes including changing their colors with changing frequency of exposed light. LC materials are useful in the pharma industry also [2–7]. This phenomenon arises from the reversible *trans*–*cis* isomerization that is induced by light irradiation, resulting in the molecular orientation of nematic LC to higher orientational entropy [8]. On the other hand, the aromatic esters are known for their thermal stability, easy synthesis, and relative resistance to the hydrolysis; in addition, the conjugation interactions of ester groups in between the two phenyl rings [9–11]. Thus, the stability of a mesophase should be greater, the greater the lateral adhesion of linear molecules which in turn would be augmented by an increase of the polarity and/or polarizability of the mesogenic portion of the molecule [12, 13]. In this respect, terminal substituents would affect the polarizability of the aromatic ring to which they are attached. This is attributed to increased intermolecular attractions with increasing polarity and polarizability of the molecule [14, 15]. Alternatively, lateral substitution increases the breadth of the laterally neat molecule, thus reducing the strength of intermolecular lateral attraction [16]. In literature, various calamitic LCs based on azo group inbuilt with ester and Schiff base linking unit were well reported [17–21].

Naoum *et al.* prepared eight homologous series based on ester and azo linking unit having methyl and fluoro group on lateral position exhibited smectic C and nematic mesophase [22]. In continue to this, Thaker and his coworkers reported various LCs based on azo ester, azo vinyl ester, and azo Schiff base derivatives [23–26]. Yoon and his coworkers studied the optical and electrical switching properties of cholesteric LCs containing azo linking group [9]. He *et al.* synthesized the chiral azo liquid crystalline terpolymer containing the cyano substituents and also studied its optical behavior by photo-induced isomerization behavior [27]. Recently, Kannan *et al.* synthesized alkoxy substituted azo cinnamate-based mesogens and further studied their photophysical behavior. In addition to this, they found the smectic C and nematic type nature in synthesized liquid crystalline azo cinnamate-based liquid crystalline compounds [28]. Yahya *et al.* prepared azo ester-based liquid crystalline acrylate compounds and study the effect of terminal substituents groups on liquid crystalline properties [29]. Ahmed *et al.* reported four-ring linked six derivatives and reported their liquid crystalline properties based on azo/ester/Schiff base group and further studied their photophysical and Density Functional Theory (DFT) study [30]. Titinchi *et al.* reported azo benzothiazole-based LCs and studied the lateral substituents on liquid crystalline properties. They studied the effect of various substituents like (-H, -OH, -CH₃, -Cl, -F) group at 3-position of the central benzene core ring [31]. After that, Naoum *et al.* reported four ring-based mesogens linked by azo ester azo group and two side substituted terminal alkoxy side groups with different side lengths and proportions. The investigation suggested the reported compounds exhibited higher mesomorphic temperature range [32]. In addition to this, Salleh and his groups prepared azo ester-based mesogens and studied the effect of lateral methyl and terminal substituents on thermal, mesomorphic, and optical properties [33]. Wang and his group reported two series of cholesteric LC polymers CPQ and CPZ series based on chiral azo LC polymethylsiloxanes with isosorbide units [34]. Very recently, El-Atawy *et al.* prepared two homologous series based on lateral nitro and azomethine linkage group [35].

In the present study, we planned to synthesize two linking group-based materials and investigated their liquid crystalline properties with understanding the effect of changing

the molecular structure by substitution at lateral and left/right terminal groups. In addition, we have also studied the optical properties of synthesized azo functionalized materials. The proposed investigation consists of the synthesis of six azo group-based mesogens with biphenyl ring and varying *n*-alkoxy left terminal group and fixed dodecyl (-OC₁₂H₂₅) tailed group at right end with the presence of nitro group on the third phenyl ring. The results obtained for the present synthesized compounds are also compared with some structurally similar series reported by our group to gain more information regarding the effect of substituents on terminal and lateral side on mesomorphic properties respectively.

2. Experimental

2.1. Materials

For the present synthesized compounds required materials: 4-hydroxy benzoic acid and 4-hydroxy acetanilide, 1-naphthol was purchased from Merck. Alkyl bromides (R-Br) were purchased from S.R.L., India. *N,N*-dimethyl aminopyridine (DMAP) and dicyclohexyl carbodiimide (DCC) were purchased from Finar Chemicals, India. The solvents were dried and purified by standard method prior to use.

2.2. Measurements

Melting points were taken on Opti-Melt (automated melting point system). The FT-IR spectra were recorded as KBr pellet on Shimadzu in the range of 3800–600 cm⁻¹. The texture images were studied on a trinocular polarizing optical microscope (POM) equipped with a heating plate and digital camera. ¹H NMR was recorded on a 400 MHz in Bruker Advance in the range of 0.5–16 ppm using CDCl₃ solvent. The phase transition temperatures were measured using Shimadzu DSC-50 at heating and cooling rates of 10 °C min⁻¹. Texture images of nematic phase were determined by the miscibility method. Thermodynamic quantities enthalpy (ΔH) and entropy ($\Delta S = \Delta H/T$) are qualitatively discussed. For the POM measurement, the newly synthesized compound is sandwiched between glass slide and coverslip and heating and cooling rate is (2 °C/min) respectively. The X-ray diffraction (XRD) measurements were performed on a Rigaku-Ultima IV powder diffractometer equipped with a Cu $k\alpha$ source ($\lambda = 1.5418 \text{ \AA}$ and 1.6 kW, X-ray tube with applied voltage and current values as 40 kV and 30 mA power) and also Philips X'PERT MPD. The absorption spectra was studied by using JASCO V-570 UV-visible recording spectrophotometer with a variable wavelength between 200 and 800 nm.

2.3. Reaction scheme

2.4. Synthesis of compounds in present series

2.4.1. 4-*n*-Alkoxy benzoic acid (A)

4-*n*-alkoxy benzoic acid is prepared by using the previously established method [36].

2.4.2. Preparation of 4-hexyloxy 3-nitro acetanilide from 4-hydroxy acetanilide (B)

4-Hexyloxy acetanilide (5 g) dissolves in 5 ml of glacial acetic acid and cooled it, add nitrating mixture and maintain the temperature up to 30 °C to 40 °C for 1 h continuing stirring. The whole mass was then added to ice-cold water and extracted with ethyl acetate. Finally, light yellow color product of 4-hydroxy 3-nitro acetanilide is obtained, filter it and crystallize in methanol solvent [37].

2.4.3. Preparation of 4-dodecyloxy 3-nitro acetanilide from 4-hydroxy 3-nitro acetanilide (C)

4-Hexyloxy 3-nitro acetanilide (0.1 mole), anhydrous K₂CO₃ (0.15 mole) and *n*-dodecyl bromide (0.15 mole) mixed in dry acetone (50 ml), reflux the reaction mixture at 3–4 h. The whole mass was then added to water and extracted with ether. Finally, off-white color product of 4-dodecyloxy 3-nitro acetanilide is obtained [37].

2.4.4. Preparation of 4-dodecyloxy 3-nitro aniline from 4-dodecyloxy 3-nitro acetanilide (D)

4-Dodecyloxy 3-nitro acetanilide (0.146 mole) taken with water (40 ml) and concentrated HCl (30 ml) were stirred for 6–7 h at 90 °C to 95 °C and then cooled to room temperature. The reaction mixture was made alkaline by the addition of 50% NaOH at 20 °C. The oily product of 4-dodecyloxy 3-nitro aniline is obtained [37].

2.4.5. Diazotization of 4-dodecyloxy 3-nitro aniline

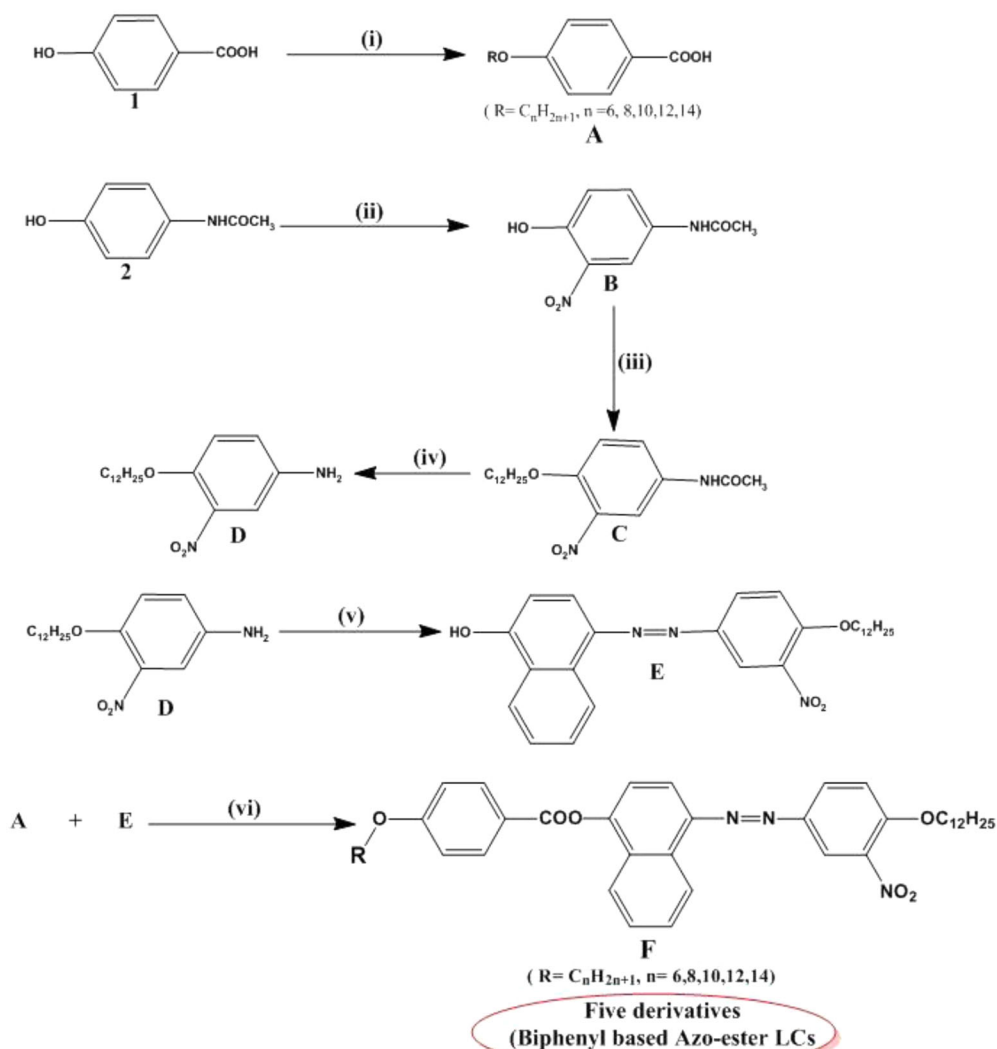
4-Dodecyloxy 3-nitro aniline (0.005 mole) was taken in a beaker containing water (10 ml). It was then cooled to 0 °C to 5 °C with ice in an ice bath. Later on, conc. HCl (0.03 mole, 3.4 ml) was added and the reaction mixture was stirred for 1 h. A solution of NaNO₂ (0.005 mole, 0.35 g) in water (5 ml) was added dropwise to the solution. The reaction mixture was stirred for 1 h. At this stage, Congo red paper turns blue and starch iodide paper also turns blue. It showed the positive test. The final diazonium salt was obtained as a clear solution, which was used for subsequent further coupling with 1-naphthol in the presence of basic medium of aqueous NaOH [37].

2.4.6. Preparation of 4-hydroxy benzyloxy naphthyl azo 4'-dodecyloxy 3'-nitrobenzene (E)

To well-stirred solution of 1-naphthol (0.005 mole, 0.81 g) in NaOH solution was added to the diazonium chloride solution of 4-dodecyloxy 3-nitro aniline for 1 h at 0–5 °C. The pH (7.0) was maintained by the addition of NaOH solution (10% w/v). The mixture was stirred for another 3–4 h for complete separation and the orange color dye was isolated by vacuum filtration which is further washed by water, dried, and purified via column chromatography performed on silica gel (60 mesh) by using the eluent of chloroform/methanol (6:4) [37].

2.4.7. Preparation of 4-*n*-alkoxy benzyloxy-naphthylazo-4'-dodecyloxy-3'-nitrobenzene (F)

The compound has been prepared by esterification of the appropriate 4-*n*-alkoxy benzoic acid (1.02 mmol) and azo dye (0.246 g, 1.02 mmol), DCC (0.457 g, 1.22 mmol), and DMAP in catalytic amount (0.002 g, 0.2 mmol) in dry CH₂Cl₂ (DCM) (30 ml) was



Scheme 1. Chemical and reagents: (i) R-Br, KOH, ethanol, reflux; (ii) Nitrating mixture; 50–60 °C, 2 h; (iii) $C_{12}H_{25}Br$, anhydrous K_2CO_3 , dry acetone, reflux 10 h; (iv) Conc.HCl, H_2O , hydrolysis, 6 h, reflux; (v) $NaNO_2$, HCl, 0–5 °C, 1-Naphthol, NaOH; (vi) DCC, DMAP, DCM, 8-h stirring at RT.

stirred at room temperature for 24 h. The white precipitate of Dicyclohexylurea (DCU) is obtained which was insulated by filtration and then remove. The resultant crude was purified by column chromatography on silica gel eluting with dichloromethane and recrystallization is carried out by using chloroform until to getting clearly transition temperatures were observed [37]. The synthetic route to a series is mentioned in Scheme 1.

2.5. Selected data of synthesized compounds

IR (KBr) in cm^{-1} for Hexyloxy (F_6), Octyloxy (F_8), Dodecyloxy (F_{10}) and Tetradecyloxy (F_{14}) derivatives:

Hexyloxy (F₆): 881 Poly methylene group of $(-\text{CH}_2-)_n$ in $-\text{OC}_6\text{H}_{13}$, 880 (-C-H- def. di-substituted on *para* side $-\text{OC}_{12}\text{H}_{25}$), 981 (-C-H- def. hydrocarbon), 1210 (-C-O-) Str, 1296, 1420, 1491 (-C-O str in $-(\text{CH}_2-)_n$ alkyl chain group), 1580 (-C-H- def. in $-\text{CH}_2$ unit in alkyl chain), 1410 ($-\text{NO}_2$ group), 1490 (-N=N-) group, 1660 (carbonyl $-\text{C}=\text{O}$ group), 1740 (-COO- ester group), 2876 and 3070 (-C-H str in CH_3).

Octyloxy (F₈): 771 and 804 Polymethylene $(-\text{CH}_2-)_n$ of $-\text{OC}_8\text{H}_{17}$ and $-\text{OC}_{12}\text{H}_{25}$, 881(-C-H- def. di-substituted-Para), 980 (-C-H- def. hydrocarbon), 1128, 1056, (-C-O-) Str, of alkyl chain, 1373, 1246 (-C-O str in $-(\text{CH}_2)_n$ alkyl chain group), 1410 ($-\text{NO}_2$ group), 1470 (-N=N- group) group, 1610 (carbonyl $-\text{C}=\text{O}$ group), 1740 (-COO- ester group), 2906 and 3036 (-C-H str in CH_3).

Dodecyloxy (F₁₂): 741 and 806 Polymethylene $(-\text{CH}_2-)_n$ of $-\text{OC}_{12}\text{H}_{25}$ and $-\text{OC}_{12}\text{H}_{25}$ group, 881 (-C-H- def. di-substituted-Para), 987 (-C-H- def. hydrocarbon in alkyl chain), 1057 (-C-O- Str.), 1290 ($-\text{C}=\text{O}$ str in $-(\text{CH}_2-)_n$ alkyl chain), 1576 (-C-H- def. in CH_2), 1410 ($-\text{NO}_2$ group), 1490 (-N=N- group), 1640 ($-\text{C}=\text{O}$ group), 1740 (-COO- ester group), 2876 and 3070 and (-C-H str in CH_3).

Tetradecyloxy (F₁₄): 760 and 871 Polymethylene $(-\text{CH}_2-)_n$ of $-\text{OC}_{14}\text{H}_{29}$ and $-\text{OC}_{12}\text{H}_{25}$, 806 (-C-H- def. di-substituted-Para side), 981 (-C-H- def. hydrocarbon in alkyl chain), 1060 (-C-O- Str.), 1210 ($-\text{C}=\text{O}$ str in $-(\text{CH}_2-)_n$ alkyl chain), 1579 (-C-H- def. in CH_2), 1410 ($-\text{NO}_2$ group), 1490 (-N=N- group), 1640 ($-\text{C}=\text{O}$ group), 1750 (-COO- ester group), 2824 and 3072 and (-C-H str in CH_3).

¹H NMR (300 MHz) in CDCl_3 (δ ppm) and ¹³C NMR (100 MHz):

Dodecyloxy (F₁₂): 0.88–0.90(t, 6H, of $-\text{OC}_{12}\text{H}_{25}$ and $-\text{OC}_{12}\text{H}_{25}$), 1.26–1.28 (m, 24H, *n*-poly methylene groups of $-\text{OC}_{12}\text{H}_{25}$ and $-\text{OC}_{12}\text{H}_{25}$), 1.76 (p, 4H, $-\text{OC}_{12}\text{H}_{25}$ and $-\text{OC}_{12}\text{H}_{25}$), 4.06 (t, 4H, $-\text{O}-\text{CH}_2-$ of $-\text{OC}_{12}\text{H}_{25}$ and $-\text{OC}_{12}\text{H}_{25}$), 7.11 (d, 2H, phenyl ring), 8.12 (d, 4H, phenyl ring), 8.62 (d, 4H, phenyl ring), 7.51 and 7.94 (d, 4H, phenyl ring), 6.84 (d, 2H, phenyl ring), 8.01 (d, 2H, phenyl ring). ¹³C NMR (100 MHz): 165.2, 164.6, 153.1, 144.4, 135.8, 130.9, 127.9, 126.0, 125.6, 122.5, 116.6, 109.7, 68.7, 53.8, 31.7, 26.1, 26.0, 14.2.

Hexyloxy (F₆): 0.88 (t, 6H, of $-\text{OC}_{12}\text{H}_{25}$ and $-\text{OC}_6\text{H}_{13}$), 1.26–1.28 (m, 16H, *n*-poly methylene groups of $-\text{OC}_{12}\text{H}_{25}$ and $-\text{OC}_6\text{H}_{13}$), 1.73 (p, 4H, $-\text{OC}_{12}\text{H}_{25}$ and $-\text{OC}_6\text{H}_{13}$), 4.04 (t, 4H, $-\text{O}-\text{CH}_2-$ of $-\text{OC}_{12}\text{H}_{25}$ and $-\text{OC}_6\text{H}_{13}$), 7.13 (d, 2H, phenyl ring), 8.01 (d, 4H, phenyl ring), 8.57 (d, 4H, phenyl ring), 7.01 and 7.68 (d, 4H, phenyl ring), 6.87 (d, 2H, phenyl ring), 6.89 (d, 2H, phenyl ring). ¹³C NMR (100 MHz): 167.2, 164.3, 149.4, 144.0, 135.6, 127.8, 126.6, 121.4, 119.4, 114.3, 109.6, 68.8, 29.8, 24.6, 15.6.

Decyloxy (F₁₀): 0.88–0.90(t, 6H, of $-\text{OC}_{12}\text{H}_{25}$ and $-\text{OC}_{10}\text{H}_{21}$), 1.26–1.28 (m, 22H, *n*-poly methylene groups of $-\text{OC}_{12}\text{H}_{25}$ and $-\text{OC}_{10}\text{H}_{21}$), 1.76 (p, 4H, $-\text{OC}_{12}\text{H}_{25}$ and $-\text{OC}_{12}\text{H}_{25}$), 4.04 (t, 4H, $-\text{O}-\text{CH}_2-$ of $-\text{OC}_{12}\text{H}_{25}$ and $-\text{OC}_{10}\text{H}_{21}$), 7.09 (d, 2H, phenyl ring), 8.21 (d, 4H, phenyl ring), 8.57 (d, 4H, phenyl ring), 7.08 and 7.91 (d, 4H, phenyl ring), 6.73 (d, 2H, phenyl ring), 8.05 (d, 2H, phenyl ring). ¹³C NMR (100 MHz): 167.2, 164.4, 149.4, 141.7, 136.4, 131.2, 125.6, 122.5, 121.6, 116.6, 114.2, 109.8, 68.7, 53.8, 31.8 26.1, 26.0, 15.2.

Octyloxy (F₈): 0.90(t, 6H, of $-\text{OC}_{12}\text{H}_{25}$ and $-\text{OC}_8\text{H}_{17}$), 1.26–1.28 (m, 18H, *n*-poly methylene groups of $-\text{OC}_{12}\text{H}_{25}$ and $-\text{OC}_8\text{H}_{17}$), 1.73 (p, 4H, $-\text{OC}_{12}\text{H}_{25}$ and $-\text{OC}_8\text{H}_{17}$), 4.04 (t, 4H, $-\text{O}-\text{CH}_2-$ of $-\text{OC}_{12}\text{H}_{25}$ and $-\text{OC}_8\text{H}_{17}$), 7.09 (d, 2H, phenyl ring), 8.10 (d, 4H, phenyl ring), 8.23 (d, 4H, phenyl ring), 7.61 (d, 4H, phenyl ring), 6.89 (d, 2H, phenyl ring), 8.03 (d, 2H, phenyl ring).

^{13}C NMR (100 MHz): 167.2, 164.8, 153.1, 141.7, 135.4, 130.6, 125.6, 122.5, 121.0, 119.7, 116.6, 114.2, 108.7, 68.7, 53.8, 31.7, 26.1, 26.0, 15.2.

3. Result and discussion

3.1. Mesomorphic behavior study

We have prepared calamitic rod-shaped optically active three phenyl ring-based azo materials and investigated their liquid crystalline properties and further compared with structurally similar homologous series. We have prepared a total of five homologous based on two linkers and one lateral group at third phenyl ring with variable side alkoxy chain on left side and fixed dodecyloxy side chain on terminal phenyl ring. At present, newly series based on ester and azo group have been synthesized by the reaction of 4-*n*-alkoxy benzoic acid (**A**) and 4-hydroxy biphenyl azo 3'-nitro 4'-dodecyloxy phenyl (azo dye) (**D**) by well-reported method [37]. The thermotropic mesophase behaviors of all the azo ester-based materials were primarily investigated by using POM, differential scanning calorimetry (DSC) analysis, and the molecular packing arrangements were further confirmed by high-temperature XRD pattern at the observed transition temperature which was observed from POM and DSC analysis. We have totally prepared five mesogens in which comp. F_6 showed only nematic phase while comp. F_8 displayed both Smectic C and nematic phase respectively. In higher chain substituted compounds (F_{10} , F_{12} , and F_{14}) showed only smectic C phase with higher mesophase stability and mesophase range. All the compounds showed mesogenic properties in heating as well as cooling conditions.

3.1.1. POM study

The transition temperatures of all six derivatives were observed by POM analysis listed in Table 1. All six derivatives showed liquid crystalline properties with higher mesophase range and stability. From the observation of the mesogenic behavior in all different materials, it can be seen that the higher alkyl side spacer substituted materials displayed lamellar type arrangement of molecules which on further heating do not pass on sliding layer and directly converted into isotropic phase without showing any nematic type molecular arrangements [11]. The formation of liquid crystalline state in materials is dependent on the number, position, and the molecular length of the side alkyl chain which increases the flexibility of molecules and also affected by the polar lateral group and various kinds of forces acting on that [11].

Table 1. Transition temperature of series-F in °C by POM.

Comp.	<i>n</i> -alkyl chain $\text{C}_n\text{H}_{2n+1}$	Transition temperatures (°C)		
		SmC	N	I
1	F_6	–	102.6	171.4
2	F_8	110.8	149.7	160.1
3	F_{10}	104.6	–	159.6
4	F_{12}	101.2	–	142.4
5	F_{14}	96.8	–	134.6

SmC = smectic C, N = nematic; I = isotropic.

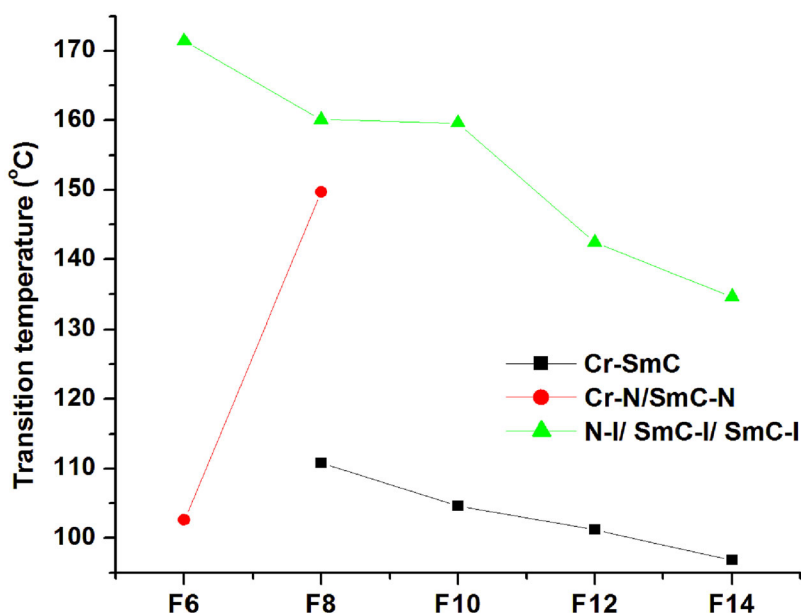


Figure 1. Mesomorphic behavior as a function of the number of carbon atoms (n) in the terminal alkoxy chain for series-F.

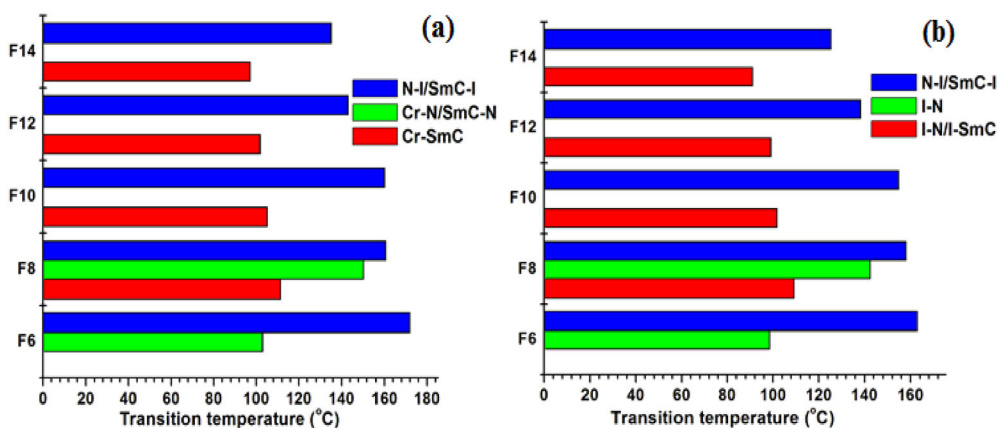


Figure 2. Bar graph of present synthesized compounds (F₆–F₁₄) on heating (a) and cooling (b).

The mesomorphic behavior of present series-F with respect to transition temperature *versus* number of variable alkoxy side chain (-OR) is shown in Fig. 1 which indicates the variation in alkyl side spacer affects the phase transition temperatures of respected compounds. Figure 1 clearly indicates the decreasing tendency with respect to lower homologous to higher homologous on heating and cooling region which basically depends on the molecular properties and thermal behavior. The decreasing tendency of the transition temperature of the compounds could be due to the lowering of the Van der Waals interactions between aromatic phenyl cores and higher degree of flexibility due to the presence of long alkyl chain in alkoxy group at left terminal part. Figure 2 indicates the bar graph of the synthesized compounds on heating and cooling condition,

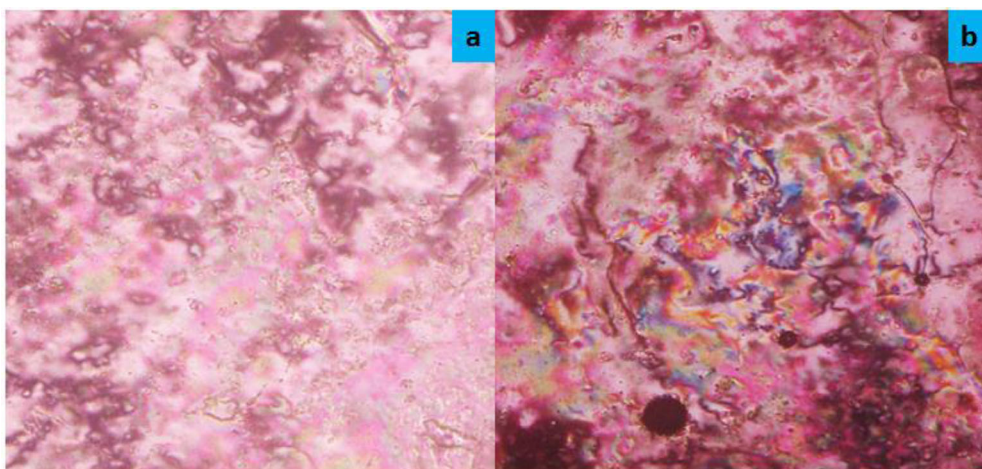


Figure 3. Optical photomicrographs on heating condition; (a) smectic C (comp.F₈) at 110.8 °C; (b) schlieren type pattern of nematic phase (comp.F₆) at 149.7 °C.

which indicates all azo mesogens showed well-order mesophase with higher temperature range.

3.1.2. Textural study

The azo-based material was sandwiched between a glass slide and a coverslip that was heated from the solid crystalline state and further cooled from the isotropic state. The POM texture image observed for compound F₆ at two different temperatures is shown in Fig. 3, respectively. The texture images of liquid crystalline compounds were observed in both heating and cooling conditions. Compound F₆ shows typical texture pattern of smectic phase at 110.8 °C on heating condition and on applying further heating up to 149.7 °C, the texture pattern is transformed into schlieren type texture pattern of nematic phase. Further, Compound F₆ showed threaded type texture pattern of smectic C phase at 102.6 °C on heating and 98.3 °C on cooling condition. Further, compound F₁₀ and F₁₂ showed needle-type texture pattern of smectic C phase at 104.6 °C and 101.2 °C on heating and at 101.2 °C and 98.6 °C on cooling condition. The texture pattern of other derivatives from the present series-F showed threaded, needle and fan type texture pattern of smectic C type phase on heating and cooling condition.

3.1.3. Comparative study

Figure 4 indicates the molecular structure of presently synthesized series-F and previously reported structural similar series by our research group [38, 39]. The first phenyl ring is substituted at left side by variable alkoxy side chain and fixed alkoxy group on right terminal end side with the addition of lateral substituent on third phenyl ring. All the series are similar with respect to phenyl core and similar linking group and induce smectic and nematic mesophase. The presence of polar flexible methylene part in variable alkoxy chain and also the presence of lateral group on the central phenyl core increases the polarity and flexibility of molecule to induce mesomorphism. The presence of the lateral substituents on third phenyl ring makes disruption and hindrance which

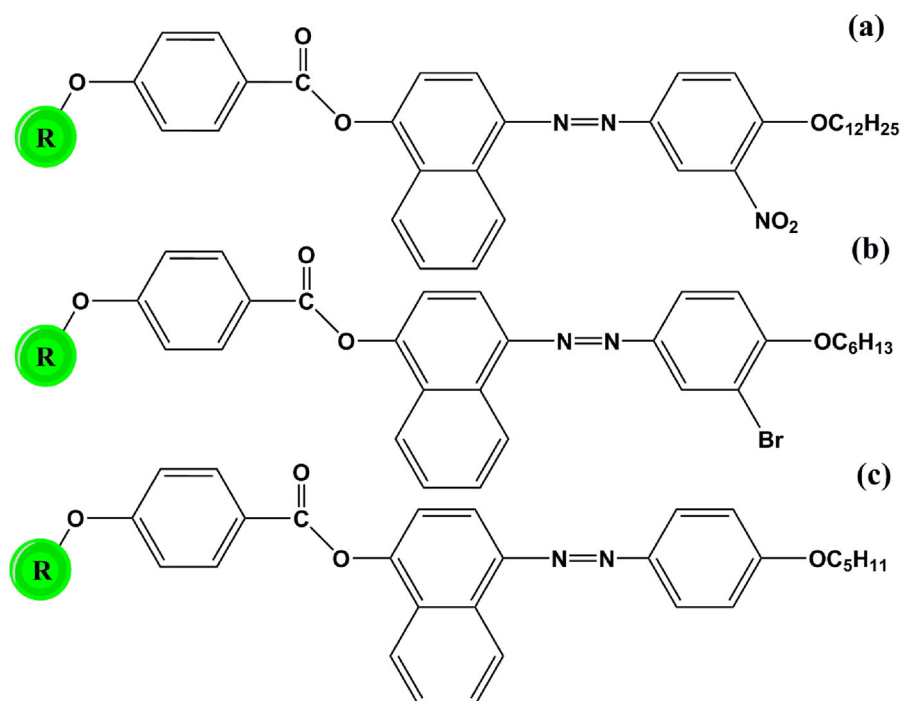


Figure 4. Molecular structure of present and similar series; series-F (a); series-1 (b); series-2 (c).

affect molecular packing arrangement and also various forces acting simultaneously which further affect mesomorphic properties. This disruption of the molecular packing is particularly advantageous for the mesomorphic and physical properties required for specific applications.

3.2. DSC study

The phase transition temperatures, enthalpies (ΔH), and entropy (ΔS) were measured by using DSC thermal analysis. All compounds are thermally stable as confirmed by the reproducibility of thermograms on second heating and cooling cycles. The DSC thermograms of comp. F_8 , F_{10} , F_{12} , and F_{14} are shown in Fig. 5. Compounds F_6 traced two endothermic peaks on second heating and cooling condition which is corresponding to solid-N and N-I phase while compound F_8 showed three endothermic peaks which belong to Cr-SmC, SmC-N and SmC-I phase transition. Comp. F_{10} displayed two endothermic peaks at 101.1°C , and 145.9°C on heating cycle and on applying cooling, it exhibited at 99.3°C and 143.7°C which is corresponding to the presence of two-phase transition. Similarly, comp. F_{12} shows two endothermic peaks at 94.2°C and 152.8°C on heating and 91.7°C and 156.6°C on cooling cycle with associated enthalpy 16.25 J/g and 12.75 J/g respectively. Comp. F_{14} showed two endothermic peaks at 92.6°C and 131.6°C on heating condition and on cooling, two peaks again reappeared at 97.7°C and 136.3°C which is further confirmed with the result obtained by POM analysis. It can be observed that the associate enthalpy of second phase transition is higher as compare to first phase transition due to the formation of crystal to mesophase in all azo-

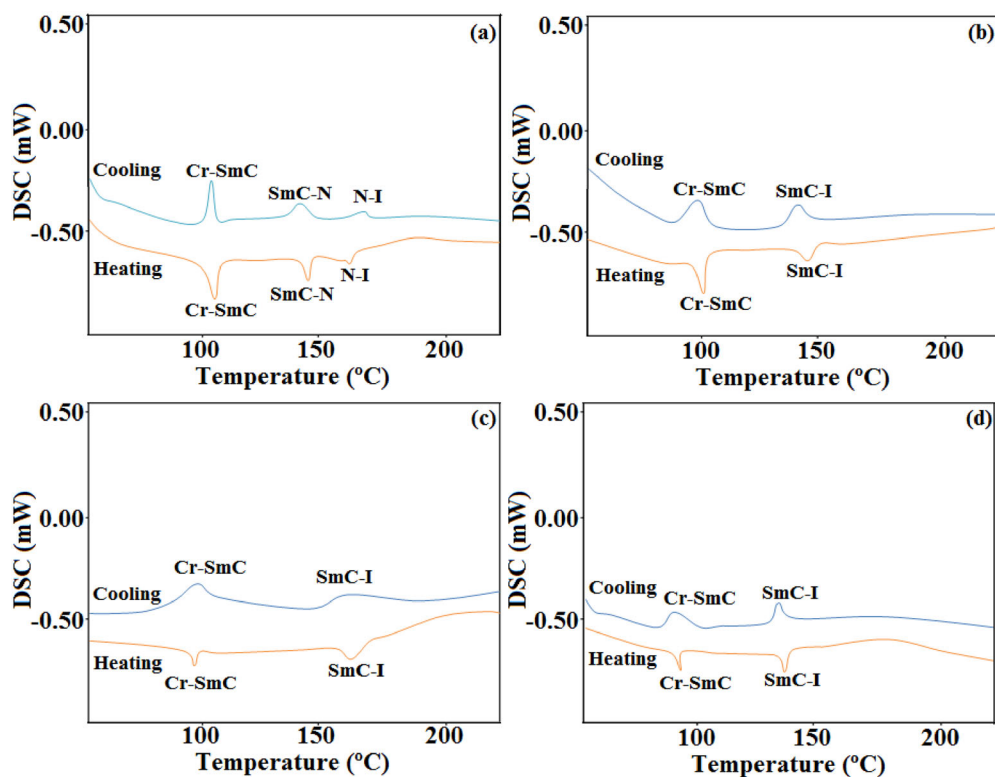


Figure 5. DSC thermograms of compound comp. F_8 (a); comp. F_{10} (b); comp. F_{12} (c) comp. F_{14} (d) on second heating and cooling cycles.

Table 2. Transition temperature ($^{\circ}\text{C}$), enthalpy (J g^{-1}), and entropy change ($\text{J g}^{-1}\text{k}^{-1}$) of compound F_6 – F_{14} by DSC measurement.

Comp.	Transition	Heating scan ($^{\circ}\text{C}$)	Cooling scan ($^{\circ}\text{C}$)	ΔH (J g^{-1})	ΔH (J g^{-1})	ΔS ($\text{J g}^{-1}\text{k}^{-1}$)	ΔS ($\text{J g}^{-1}\text{k}^{-1}$)
F_6	Cr-N	107.4	101.7	14.78	11.86	0.0388	0.0316
	N-I	172.3	169.3	11.21	10.76	0.0251	0.0243
F_8	Cr-SmC	104.3	102.9	7.54	8.23	0.0199	0.0216
	SmC-N	142.1	138.2	10.58	12.96	0.0254	0.0315
	N-I	163.9	157.3	8.23	9.86	0.0188	0.0229
F_{10}	Cr-SmC	101.1	99.3	9.45	14.68	0.0252	0.0394
	SmC-I	145.9	143.7	6.83	12.54	0.0163	0.0300
F_{12}	Cr-SmC	94.2	91.7	16.25	8.52	0.0442	0.0233
	SmC-I	152.8	156.6	12.75	7.64	0.0299	0.0177
F_{14}	Cr-SmC	92.6	97.7	10.48	19.54	0.0286	0.0527
	SmC-I	131.6	136.3	9.26	14.02	0.0228	0.0342

Cr-SmC = solid to SmC; SmC-I = SmC to isotropic; Cr-N = solid to nematic; N-I = nematic to isotropic.

based derivatives which confirm the liquid crystalline properties with good stability as well. The phase transition temperatures, enthalpy, and entropy values for the present synthesized series are summarized in Table 2.

3.3. XRD analysis

To investigate the molecular arrangement in azo-based mesogens for further confirmation to observed smectic and nematic phase, we have performed to perform a high-

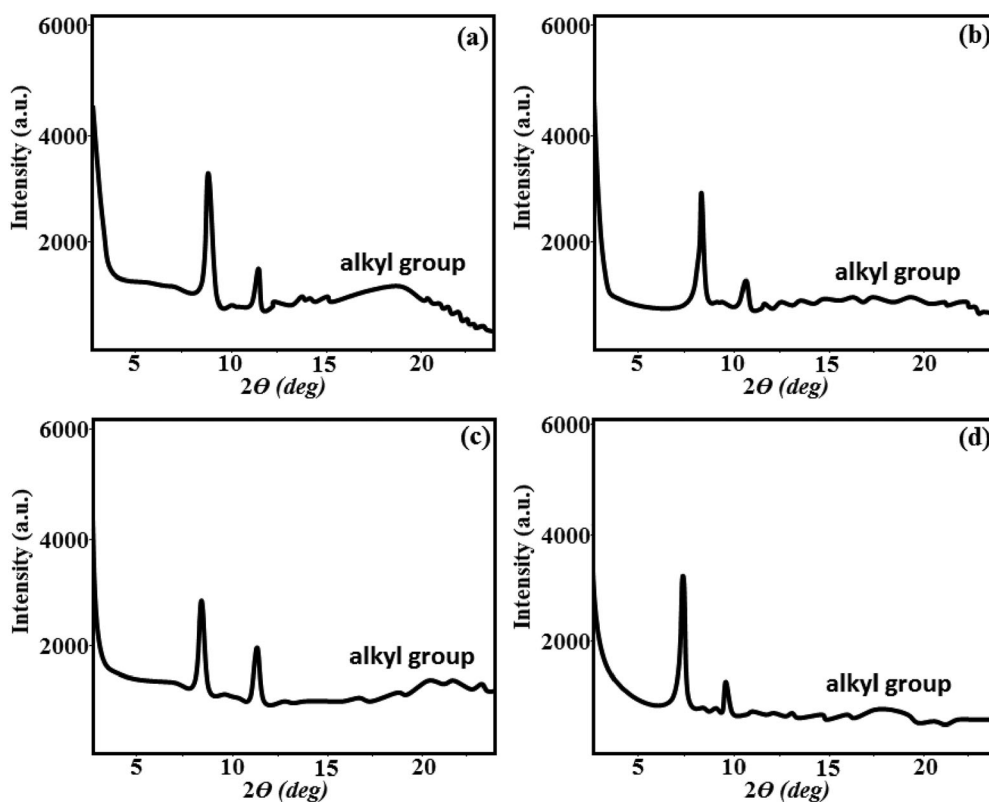


Figure 6. XRD traces of compound F_8 (a); F_{10} (b); F_{12} (c); F_{14} (d) measured at transition temperature.

temperature XRD to correlate with the results obtained from DSC and POM analysis. The XRD data of comp. F_8 , F_{10} , F_{12} , and F_{14} are shown in Fig. 6. According to the graphical proposed molecular arrangement in smectic C as well nematic phase, the molecules are arranged in lamellar order, although, the long axes of the molecules are tilted to the layers' planes shown in Fig. 7. Figure 6 clearly indicates the X-ray pattern of compound F_8 showed the diffraction peaks in the small-angle diffraction region corresponded to the smectic arrangement. The reflections for the small-angle area correspond to a smectic layer type arrangement of present synthesized azo-based mesogens. The reflection and d -spacing observed for compound F_8 at $2\theta = 8.8^\circ$, 11.6° , 22.6° are 9.71 \AA , 6.27 \AA , 3.42 \AA which confirms the lamellar packing of molecules in smectic type arrangement. Compound F_{10} at $2\theta = 8.3^\circ$, 11.4° , 23.1° showed d -spacing at 10.67 \AA , 7.79 \AA , and 3.43 \AA . Further, compound F_{12} showed mainly two reflections at 8.1° and 10.9° in small and one trace peak at 24.6° having corresponding d -spacing value 10.92 \AA , 8.14 \AA , and 3.43 \AA , respectively. Similarly, compound F_{14} showed two main reflection peaks at 7.4° , 9.8° , and 23.4° with d -spacing value as 11.96 \AA , 9.04 \AA , and 3.42 \AA . The presence of variable alkyl chain in alkoxy terminal side group in octyl (F_8), dodecyl (F_{12}), and tetradecyl (F_{14}) may increase the arrangement of molecules in ordering layered and formation of molecules in smectic mesophase. The reflection peak appeared at higher angle region is due to the presence of alkyl chain interaction. Further, the observed d -spacing length of respected compounds is nearly matched with

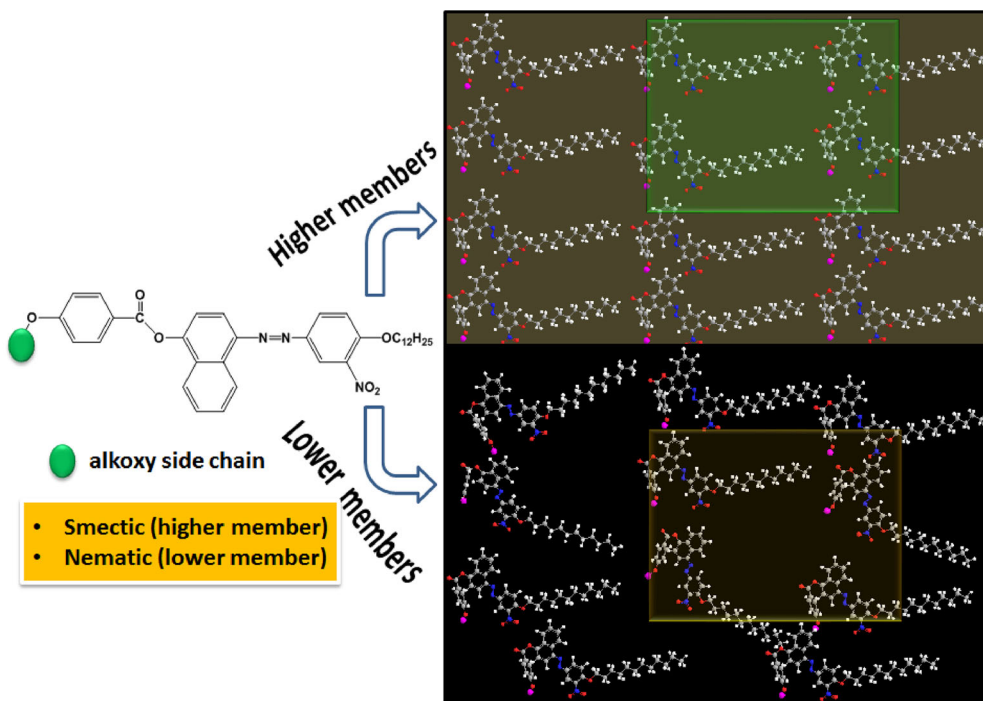


Figure 7. Representation of molecular packing in smectic and nematic mesophase in present series-F.

the calculated length of the molecules respectively. The XRD results indicate the molecular arrangement of molecules may be just a smectic organization which is further revealed with POM and DSC results.

3.4. Optical properties

Figure 8 represents the UV-Vis absorption spectra of presently synthesized azo-based materials (F_6 , F_8 , F_{10} , and F_{14}) are recorded in dichloromethane solution. The azo-based mesogens were irradiated with UV light, the band corresponding to both $\pi-\pi^*$ and $n-\pi^*$ transitions which decrease with increasing irradiation time period [28]. The observed bands corresponding to isomerize product increase by increasing the irradiation time, which confirmed the presence of photoisomerization effect at various time intervals has occupied in the range of 364–551 nm. One can see that all the spectra of four corresponding compounds are characterized by the two absorption peaks with the maxima at 294 and 374 nm. The appearing of low intense short-wavelength absorption maxima appeared at nearly 294 and 281 nm due to the presence of $\pi-\pi^*$ transition of phenyl rings. However, the highly intense longer wavelength absorption maxima observed at 374 and 388 nm due to the presence of a $\pi-\pi^*$ transition involving the π -electronic system throughout the whole mesogenic portion, with a considerable charge transfer character [28]. Compound F_6 irradiated at 378 nm, for the study of *E-Z* isomerization, the decrease in the absorption band to 363 nm is ascribed to $\pi-\pi^*$ transition of the *trans* (*E*) isomer basically observed in azo ($-N=N-$) group. In higher region with time interval, a weak absorption band found in the visible region around 484 nm

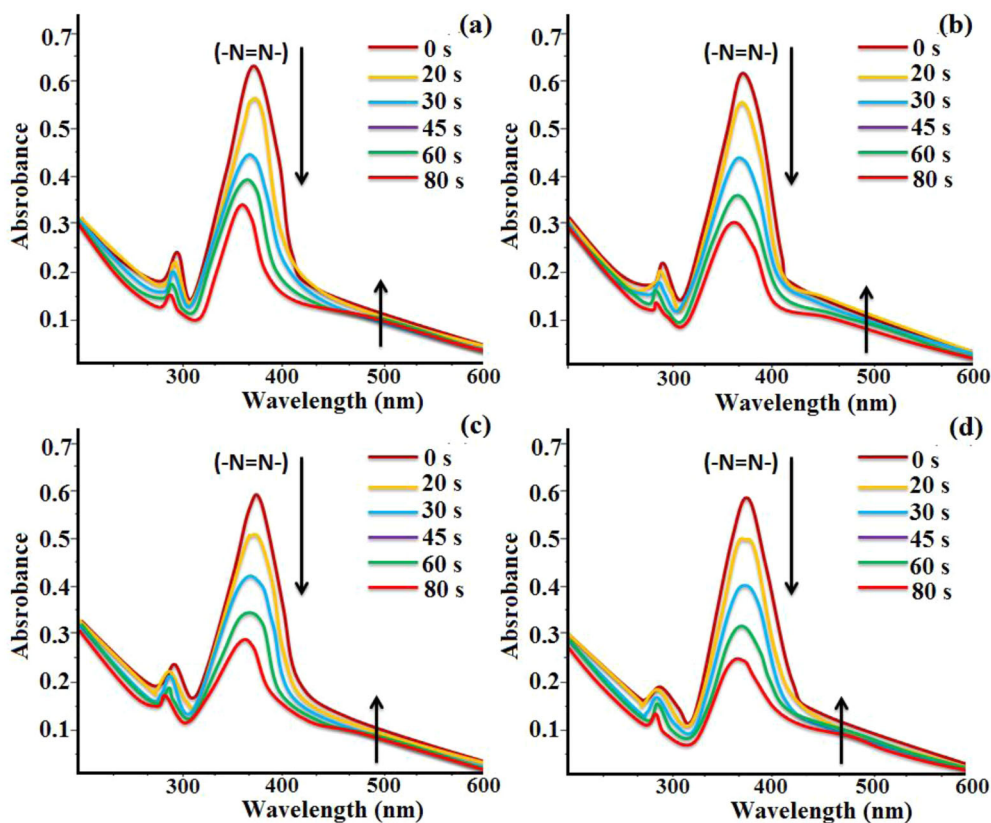


Figure 8. Absorption spectrum of compound F_6 (a); F_8 (b); F_{10} (c); F_{14} (d).

which represents to $n-\pi^*$ transition of *cis* (*Z*) isomer in the azo group was gradually increased by reaching photo stationary state at 80 s. After that, no change observed in the absorption spectrum which is further confirmed the photo-saturation of *E-Z* (*trans-cis*) isomerization process. In addition to this, compound F_8 irradiated at 376 nm, again *E-Z* isomerization is taking place which further decreases up to 361 nm is ascribed to $\pi-\pi^*$ transition of the *trans* (*E*) isomer and very weak absorption band found in the visible region around at 479 nm which confirms the appearance of $n-\pi^*$ transition of *cis* (*Z*) isomer. Further, compound F_{10} and F_{14} irradiated at 383 nm and 388 nm which is decreased due to the formation of *E-Z* isomerization at 357 nm and 363 nm due to $\pi-\pi^*$ transition of the *trans* isomer (*E*) and also exhibiting the weak absorption peak at 483 nm and 489 nm, this is due to the formation of $n-\pi^*$ transition of *cis* (*Z*) isomer, respectively. **Figure 9** shows the *trans* and *cis* isomer of azo ester-based present synthesized derivatives which clearly indicated that the photoisomerization is taking place.

3.5. Frontier molecular orbital (FMO) distribution

The distribution of FMO of final target ester azo group-based comp. F_6 (series-F) and comp. F_{14} are shown in **Fig. 10**. In this, we have compared the effect on band gap over

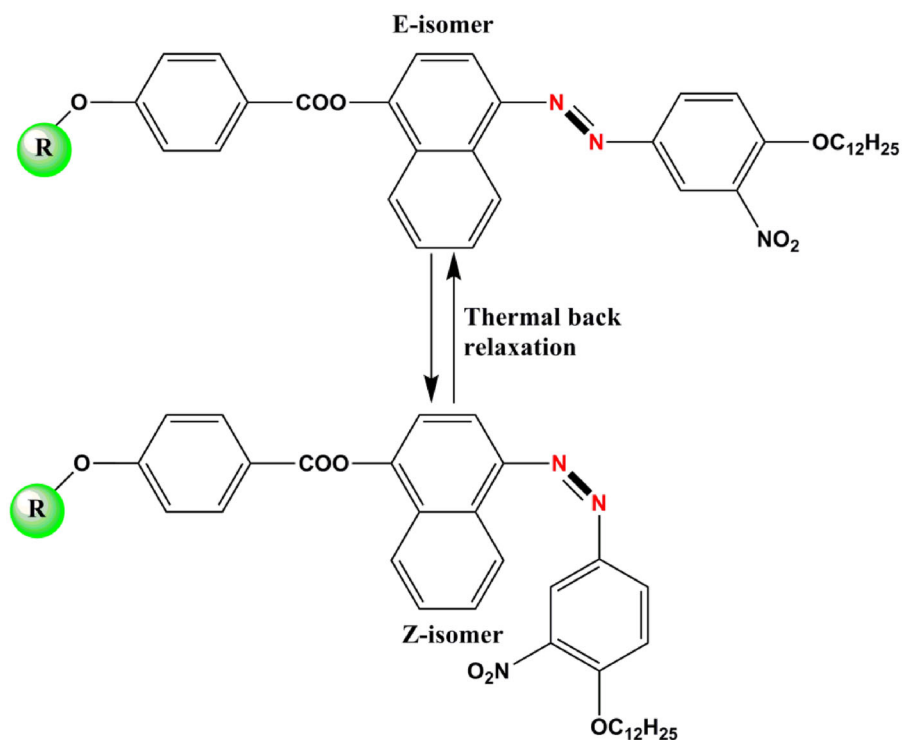


Figure 9. Schematic representation of the *trans-cis* transition of the azo-based mesogens (five derivatives).

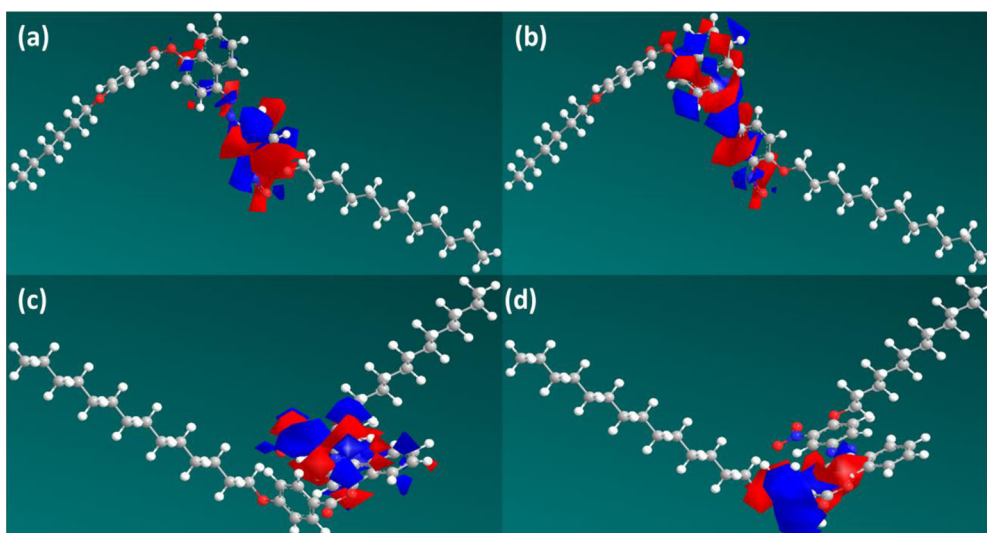


Figure 10. FMO distribution of comp. F_6 (HOMO, series-F) (a); comp. F_6 (LUMO, series-F) (b); comp. F_{14} (HOMO, series-F) (c); comp. F_{14} (LUMO, series-F).

the substitution on azo dye (**E**) to achieve final liquid crystalline materials (F_6 , F_{14}) (Fig. 10). A close examination of these orbitals reveals that the HOMO (highest occupied molecular orbital) is predominantly localized on the third phenyl ring over azo

Table 3. Average thermal stability in °C.

Series	Series-F	Series-1	Series-2
SmC-I	145.5	146.9	142.5
Cr-SmC	103.3	114.4	99.77
N-I	165.7	154.6	119.21
SmC-N	149.7	147.6	141.4

SmC-I = smectic C to isotropic; Cr-N = solid to nematic; Cr-SmC = solid to smectic C; N-I = nematic to isotropic.

linking unit while the LUMO (lowest unoccupied molecular orbital) is mostly concentrated on second phenyl and third phenyl ring over azo group. It clearly indicates that the substitution of flexible alkyl chain on both the terminal side group does not affect influence on the HOMO–LUMO orbital distributions. The band gap calculated for both the target compounds (F_6 , F_{14}) is found to be lower than one which clearly indicates the higher reactivity of the compounds. The presence of nitro group on third phenyl ring provides more electron density, polarity which provide more charge transfer of electron over the central azo functionalized group further reduces the resonance effect caused by phenyl core, as a result the HOMO–LUMO energy gap or band gap (E_g) is reduced with respect to other similar reported azo ester-based mesogenic materials. Thus, it can be concluded that the electronic properties of present synthesized compounds could have originated from the phenylic-azo group rather than other linking units.

3.6. Thermal stability and temperature range of mesophase

Thermal stability of present novel synthesized series-F is further compared with structurally similar series-1 and series-2 are listed in Table 3, respectively. The present synthesized series-F displayed higher thermal stability of nematic to isotropic and smectic C to nematic phase with good mesophase temperature range as compared to series-1 and series-2. The geometrical structures of all three series are the same except terminal and lateral groups to induce smectic and nematic phases. In present series-F which contains azo ester linking group and fixed $-OC_{12}H_{25}$ group on right terminal end with the presence of nitro group which affect its polarity, polarizability and also affect the linearity of the molecules causes higher mesophase thermal stability as compared to series-1 and series-2. Previously reported series-2 showed lower stability and mesophase temperature range as compared to other series due to its planarity structure without any lateral substituent groups, as a result, the mesophase commences early from C_4 homologue and continue to exhibit liquid crystalline properties till the last C_{18} homologue [38, 39].

Fig. 11 represents the proposed mechanism to indicate the arrangement of azo-based mesogens in both lamellar packing (SmC) and on further heating transform into nematic phase (N) before passing to the isotropic phase transition. All the derivatives showed good E-Z isomerization with good temperature and stability of mesophase. In addition, we have compared the structural arrangement of lower side alkyl chain substituted compounds which showed nematic mesophase and higher alkyl chain substituted compounds that exhibited SmC phase. All the compounds showed mesophase on heating and cooling conditions with the addition of good photophysical behavior as well.

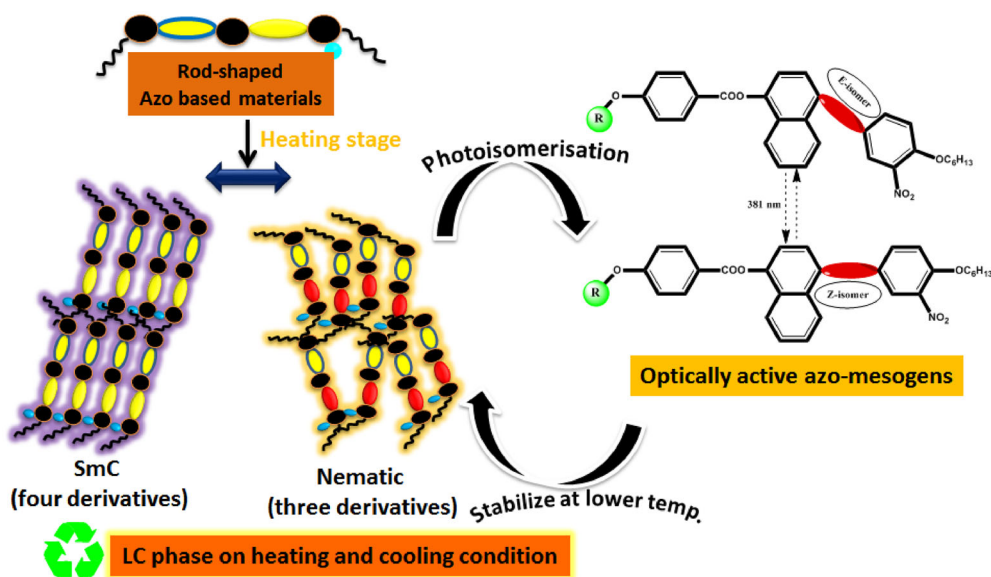


Figure 11. Propose mechanism of present series-F.

4. Conclusion

A new optically active azo ester-based mesogens based on two phenyl and one naphthyl cores with variable alkoxy side chain and lateral nitro group has been synthesized and well characterized by various spectroscopic techniques. The liquid crystalline properties of the synthesized mesogens are carried out by POM, DSC, and high-temperature XRD techniques, and the photophysical behaviors are studied by UV-Vis spectroscopy technique. In the present nitro-based azo functionalized series, lower members showed smectic C and nematic phase while higher members displayed only smectic C mesophase. The observed mesophase in the present series is enantiotropically in nature. The thermal stability and mesophase temperature range are influenced by the lateral substituted nitro group in series-F which further compares with well-reported azo-based homologous series. The group efficiency order derived on the basis of (a) observed mesophase thermal stability, (b) early or late commencement of mesophase, (c) temperature range of mesophase. The HOMO-LUMO calculations indicate the lower band gap of target compounds which showed good reactivity and lower stability with addition by intermolecular charge transfer interactions and revealed the electronic properties of present synthesized azo mesogens were originated from first and second phenyl ring inbuilt with ester and azo group and also studied the effect of lateral nitro on electron charge transfer and reactivity. The duration required for exhibiting photoisomerization phenomena mainly related to the chemical structure of the target compounds.

Acknowledgments

A.T., D.D., V.D., and R.B.P. acknowledge thanks to K.K. Jarodwala Maninagar Science College, Gujarat University, Ahmedabad for providing research lab and other facilities. V.S. also acknowledges thanks to Department of Chemistry, Faculty of Basic and Applied Science, Sirohi,

Rajasthan for providing some instrument and lab facility. The authors are also thankful to NFDD Centre Rajkot, IIT Mandi, Sourashtra University, MLSU University, and MNIT Jaipur for providing spectral and other services.

References

- [1] T. H. Sie, G. Yeap, and P. L. Boey, *Aust. J. Basic Appl. Sci.* **3** (4), 3417 (2009).
- [2] H. M. Shukla *et al.*, *J. Chem. Pharm. Res.* **2** (5), 169 (2010).
- [3] E. Smela, *Adv. Mater.* **15** (6), 481 (2003). doi:10.1002/adma.200390113
- [4] M. Vijay Srinivasan and P. Kannan, *J. Mater. Sci.* **46** (15), 5029 (2011). doi:10.1007/s10853-011-5423-x
- [5] G. Hegde *et al.*, *J. Mater. Chem. C* **1** (22), 3600 (2013). doi:10.1039/c3tc00921a
- [6] A. V. Doshi, U. C. Bhoya, and J. J. Travadi, *Mol. Cryst. Liq. Cryst.* **552** (1), 10 (2012). doi:10.1080/15421406.2011.591663
- [7] U. C. Bhoya, N. N. Vyas, and A. V. Doshi, *Mol. Cryst. Liq. Cryst.* **552** (1), 104 (2012). doi:10.1080/15421406.2011.604590
- [8] M. Vijay Srinivasan, P. Kannan, and A. Roy, *New J. Chem.* **37** (5), 1584 (2013). doi:10.1039/c3nj41030g
- [9] S. W. Oh *et al.*, *RSC Adv.* **7** (32), 19497 (2017). doi:10.1039/C7RA01507K
- [10] V. S. Sharma *et al.*, *Liq. Cryst. Today* **26** (3), 46 (2017). doi:10.1080/1358314X.2017.1359401
- [11] V. S. Sharma and R. B. Patel, *Mol. Cryst. Liq. Cryst.* **630** (1), 58 (2016). doi:10.1080/15421406.2016.1146866
- [12] V. S. Sharma and R. B. Patel, *Mol. Cryst. Liq. Cryst.* **643** (1), 1 (2017). doi:10.1080/15421406.2016.1262672
- [13] Y. Kim *et al.*, *Liq. Cryst.* **45** (5), 757 (2018). doi:10.1080/02678292.2017.1382582
- [14] A. Ranjkesh *et al.*, *RSC Adv.* **8** (40), 22835 (2018). doi:10.1039/C8RA03701A
- [15] W. Haase and H. Wedel, *Mol. Cryst. Liq. Cryst.* **38** (1), 61 (1977). doi:10.1080/15421407708084375
- [16] J. Goodby *et al.*, *Physical Properties of Liquid Crystals* (Wiley-VCH, Weinheim, Germany, 1999).
- [17] X. Zhu *et al.*, *RSC Adv.* **7** (73), 46344 (2017). doi:10.1039/C7RA06958H
- [18] E. Westphal, I. H. Bechtold, and H. Gallardo, *Macromolecules* **43** (3), 1319 (2010). doi:10.1021/ma902460c
- [19] C. Selvarasu and P. Kannan, *J. Mol. Struct.* **1125**, 234 (2016). doi:10.1016/j.molstruc.2016.06.081
- [20] M. Sarigul *et al.*, *J. Mol. Struct.* **1149**, 520 (2017). doi:10.1016/j.molstruc.2017.08.016
- [21] G. Ozkan *et al.*, *Spectrochim. Acta, Part A.* **150**, 966 (2015). doi:10.1016/j.saa.2015.06.038
- [22] M. M. Naoum *et al.*, *Liq. Cryst.* **44** (11), 1664 (2017). doi:10.1080/02678292.2017.1306886
- [23] B. T. Thaker and J. B. Kanojiya, *Liq. Cryst.* **38** (8), 1035 (2011). doi:10.1080/02678292.2011.594525
- [24] B. T. Thaker *et al.*, *Liq. Cryst.* **40** (2), 237 (2013). doi:10.1080/02678292.2012.737478
- [25] B. T. Thaker, J. B. Kanojiya, and R. S. Tandel, *Mol. Cryst. Liq. Cryst.* **528** (1), 120 (2010). doi:10.1080/15421406.2010.504632
- [26] U. C. Makwana *et al.*, *Liq. Cryst.* **40**, 237 (2012).
- [27] H. W. Zhao *et al.*, *Liq. Cryst.* **44** (14–15), 2379 (2017). doi:10.1080/02678292.2017.1335894
- [28] C. Selvarasu and P. Kannan, *Mol. Cryst. Liq. Cryst.* **648** (1), 77 (2017). doi:10.1080/15421406.2017.1301859
- [29] M. R. Karim *et al.*, *Liq. Cryst.* **43** (12), 1862 (2016). doi:10.1080/02678292.2016.1216620
- [30] N. H. S. Ahmed *et al.*, *RSC Adv.* **10** (16), 9643 (2020). doi:10.1039/C9RA10499B
- [31] U. J. A. Hamdani *et al.*, *Liq. Cryst.* **47** (14–15), 2257 (2020). doi:10.1080/02678292.2020.1766134
- [32] A. M. Abdelrahman *et al.*, *Liq. Cryst.* **47** (12), 1772 (2020). doi:10.1080/02678292.2020.1727035

- [33] S. N. F. Sardon *et al.*, *J. Mol. Struct.* **1225**, 129112 (2021). doi:[10.1016/j.molstruc.2020.129112](https://doi.org/10.1016/j.molstruc.2020.129112)
- [34] Y. R. Ma *et al.*, *Liq. Cryst.* **47** (5), 702 (2020). doi:[10.1080/02678292.2019.1673843](https://doi.org/10.1080/02678292.2019.1673843)
- [35] M. A. El-Atawy *et al.*, *Molecules* **26** (7), 1927 (2021). doi:[10.3390/molecules26071927](https://doi.org/10.3390/molecules26071927)
- [36] V. S. Sharma, A. S. Sharma, and R. B. Patel, *Mol. Cryst. Liq. Cryst.* **556**, 32 (2017).
- [37] V. S. Sharma, A. P. Shah, and A. S. Sharma, *New J. Chem.* **43** (8), 3556 (2019). doi:[10.1039/C8NJ04997A](https://doi.org/10.1039/C8NJ04997A)
- [38] U. H. Jadeja *et al.*, *Mol. Cryst. Liq. Cryst.* **680** (1), 46 (2019). doi:[10.1080/15421406.2019.1627091](https://doi.org/10.1080/15421406.2019.1627091)
- [39] U. H. Jadeja *et al.*, *Mol. Cryst. Liq. Cryst.* **630** (1), 144 (2016). doi:[10.1080/15421406.2016.1146935](https://doi.org/10.1080/15421406.2016.1146935)